CLNS 05/1945
CLEO 05-31

Measurement of $\Gamma_{ee}(J/\psi)$, $\Gamma_{\rm tot}(J/\psi)$, and $\Gamma_{ee}[\psi(2S)]/\Gamma_{ee}(J/\psi)$

G. S. Adams,[1] M. Anderson,[1] J. P. Cummings,[1] I. Danko,[1] J. Napolitano,[1] Q. He,[2] J. Insler,[2] H. Muramatsu,[2] C. S. Park,[2] E. H. Thorndike,[2] T. E. Coan,[3] Y. S. Gao,[3] F. Liu,[3] R. Stroynowski,[3] M. Artuso,[4] S. Blusk,[4] J. Butt,[4] J. Li,[4] N. Menaa,[4] R. Mountain,[4] S. Nisar,[4] K. Randrianarivony,[4] R. Redjimi,[4] R. Sia,[4] T. Skwarnicki,[4] S. Stone,[4] J. C. Wang,[4] K. Zhang,[4] S. E. Csorna,[5] G. Bonvicini,[6] D. Cinabro,[6] M. Dubrovin,[6] A. Lincoln,[6] D. M. Asner,[7] K. W. Edwards,[7] R. A. Briere,[8] J. Chen,[8] T. Ferguson,[8] G. Tatishvili,[8] H. Vogel,[8] M. E. Watkins,[8] J. L. Rosner,[9] N. E. Adam,[10] J. P. Alexander,[10] K. Berkelman,[10] D. G. Cassel,[10] J. E. Duboscq,[10] K. M. Ecklund,[10] R. Ehrlich,[10] L. Fields,[10] R. S. Galik,[10] L. Gibbons,[10] R. Gray,[10] S. W. Gray,[10] D. L. Hartill,[10] B. K. Heltsley,[10] D. Hertz,[10] C. D. Jones,[10] J. Kandaswamy,[10] D. L. Kreinick,[10] V. E. Kuznetsov,[10] H. Mahlke-Krüger,[10] T. O. Meyer,[10] P. U. E. Onyisi,[10] J. R. Patterson,[10] D. Peterson,[10] E. A. Phillips,[10] J. Pivarski,[10] D. Riley,[10] A. Ryd,[10] A. J. Sadoff,[10] H. Schwarthoff,[10] X. Shi,[10] S. Stroiney,[10] W. M. Sun,[10] T. Wilksen,[10] M. Weinberger,[10] S. B. Athar,[11] P. Avery,[11] L. Breva-Newell,[11] R. Patel,[11] V. Potlia,[11] H. Stoeck,[11] J. Yelton,[11] P. Rubin,[12] C. Cawlfield,[13] B. I. Eisenstein,[13] I. Karliner,[13] D. Kim,[13] N. Lowrey,[13] P. Naik,[13] C. Sedlack,[13] M. Selen,[13] E. J. White,[13] J. Wiss,[13] M. R. Shepherd,[14] D. Besson,[15] T. K. Pedlar,[16] D. Cronin-Hennessy,[17] K. Y. Gao,[17] D. T. Gong,[17] J. Hietala,[17] Y. Kubota,[17] T. Klein,[17] B. W. Lang,[17] R. Poling,[17] A. W. Scott,[17] A. Smith,[17] S. Dobbs,[18] Z. Metreveli,[18] K. K. Seth,[18] A. Tomaradze,[18] P. Zweber,[18] J. Ernst,[19] H. Severini,[20] S. A. Dytman,[21] W. Love,[21] S. Mehrabyan,[21] V. Savinov,[21] O. Aquines,[22] Z. Li,[22] A. Lopez,[22] H. Mendez,[22] J. Ramirez,[22] G. S. Huang,[23] D. H. Miller,[23] V. Pavlunin,[23] B. Sanghi,[23] I. P. J. Shipsey,[23] and B. Xin[23]

(CLEO Collaboration)

[1]*Rensselaer Polytechnic Institute, Troy, New York 12180*
[2]*University of Rochester, Rochester, New York 14627*
[3]*Southern Methodist University, Dallas, Texas 75275*
[4]*Syracuse University, Syracuse, New York 13244*
[5]*Vanderbilt University, Nashville, Tennessee 37235*
[6]*Wayne State University, Detroit, Michigan 48202*
[7]*Carleton University, Ottawa, Ontario, Canada K1S 5B6*
[8]*Carnegie Mellon University, Pittsburgh, Pennsylvania 15213*
[9]*Enrico Fermi Institute, University of Chicago, Chicago, Illinois 60637*
[10]*Cornell University, Ithaca, New York 14853*
[11]*University of Florida, Gainesville, Florida 32611*
[12]*George Mason University, Fairfax, Virginia 22030*
[13]*University of Illinois, Urbana-Champaign, Illinois 61801*
[14]*Indiana University, Bloomington, Indiana 47405*
[15]*University of Kansas, Lawrence, Kansas 66045*
[16]*Luther College, Decorah, Iowa 52101*
[17]*University of Minnesota, Minneapolis, Minnesota 55455*
[18]*Northwestern University, Evanston, Illinois 60208*
[19]*State University of New York at Albany, Albany, New York 12222*
[20]*University of Oklahoma, Norman, Oklahoma 73019*

arXiv:hep-ex/0512046v3 6 Apr 2006

[21] *University of Pittsburgh, Pittsburgh, Pennsylvania 15260*
[22] *University of Puerto Rico, Mayaguez, Puerto Rico 00681*
[23] *Purdue University, West Lafayette, Indiana 47907*
(Dated: December 16, 2005)

Abstract

Using data acquired with the CLEO detector at the CESR e^+e^- collider at $\sqrt{s} = 3.773$ GeV, we measure the cross section for the radiative return process $e^+e^- \to \gamma J/\psi$, $J/\psi \to \mu^+\mu^-$, resulting in $\mathcal{B}(J/\psi \to \mu^+\mu^-) \times \Gamma_{ee}(J/\psi) = 0.3384 \pm 0.0058 \pm 0.0071$ keV, $\Gamma_{ee}(J/\psi) = 5.68 \pm 0.11 \pm 0.13$ keV, and $\Gamma_{\rm tot}(J/\psi) = 95.5 \pm 2.4 \pm 2.4$ keV, in which the errors are statistical and systematic, respectively. We also determine the ratio $\Gamma_{ee}[\psi(2S)]/\Gamma_{ee}(J/\psi) = 0.45 \pm 0.01 \pm 0.02$.

The full and dileptonic widths of a hadronic resonance, $\Gamma_{\rm tot}$ and Γ_{ee}, describe fundamental properties of the strong potential [1]. The value of Γ_{ee} for a particular resonance is, in principle, predictable within QCD, although the strong interaction effects in the quark-antiquark pair annihilation make calculations challenging. Heavy quarkonia offer the best testing ground for lattice-based (LQCD) techniques [2], and a fortuitous convergence in precision to the few percent level is occuring on both the theoretical and experimental fronts. In 2003, BaBar measured $\mathcal{B}_{\mu\mu} \times \Gamma_{ee}$ [3], where $\mathcal{B}_{\mu\mu} \equiv \mathcal{B}(J/\psi \to \mu^+\mu^-)$, using the novel technique of counting radiative returns from e^+e^- collisions at $\sqrt{s} = 10.58$ GeV. This allowed the world average [4] uncertainty on $\Gamma_{ee}(J/\psi)$ and $\Gamma_{\rm tot}(J/\psi)$ to be reduced by nearly a factor of two when combined with a BES [5] determination of the J/ψ dileptonic branching fraction $\mathcal{B}_{\ell\ell}$, which has a relative 1.7% uncertainty. At the same time, progress on predicting and measuring dielectronic widths of bottomonium [2, 6] is occuring, providing further checks of LQCD computations. For the Υ system, the LQCD predictions for the ratios $\Gamma_{ee}[\Upsilon(nS)]/\Gamma_{ee}[\Upsilon(1S)]$ are expected to be more accurate than those of the absolute individual widths.

In this Article we describe a measurement of the J/ψ full and dielectronic widths with CLEO-c data from e^+e^- collisions near the peak of the $\psi(3770)$ resonance. The method is similar to that used earlier by BaBar [3] and in CLEO's recent measurement [7] of $\Gamma_{ee}[\psi(2S)]$: we select $\mu^+\mu^-(\gamma)$ events, each with a dimuon mass in the general region of the J/ψ, and count the excess over non-resonant QED production, $e^+e^- \to \gamma\mu^+\mu^-$. (The e^+e^- final state is not used due to the large t-channel contribution, which limits the attaintable statistical precision relative to $\mu^+\mu^-$). The J/ψ component will peak at $M(\mu^+\mu^-)$=$M_{J/\psi}$ with a mass resolution dominated by detector effects. The cross section for the excess is proportional to $\mathcal{B}_{\mu\mu} \times \Gamma_{ee}(J/\psi)$. Assuming lepton universality, we can then divide by CLEO's own $\mathcal{B}_{\ell\ell}$ [8], with a relative accuracy of 1.18%, once to obtain $\Gamma_{ee}(J/\psi)$ and once more for $\Gamma_{\rm tot}(J/\psi)$.

We use e^+e^- collision data collected with the CLEO detector [9] acquired at a center-of-mass energy $\sqrt{s_0}$=3.773 GeV at the Cornell Electron Storage Ring (CESR) [10]. The CLEO detector features a solid angle coverage of 93% for charged and neutral particles. The charged particle tracking system operates in a 1.0 T magnetic field along the beam axis and achieves a momentum resolution of ~0.6% at momenta of 1 GeV/c. The integrated luminosity ($\mathcal{L}$) was measured using e^+e^-, $\gamma\gamma$, and $\mu^+\mu^-$ events [11] and normalized with a Monte Carlo (MC) simulation based on the Babayaga [12] generator combined with GEANT-based [13] detector modeling. Results from the three final states are consistent and together yield $\mathcal{L} = 280.7 \pm 2.8$ pb^{-1}.

The differential cross section for $e^+e^- \to \gamma J/\psi \to \gamma\mu^+\mu^-$ can be expressed [14, 15, 16] in terms of the e^+e^- invariant mass s, the dimuon mass-squared s', and the variable $x \equiv (1 - s'/s)$ as

$$\frac{d\sigma}{dx}(s,x) = W(s,x) \times b(s') \times \Gamma_{ee} \times \mathcal{B}_{\mu\mu} \quad , \tag{1}$$

where $W(s,x)$ is the initial state radiation (ISR) γ-emission probability, $b(s')$ is the relativistic Breit-Wigner function, and Γ_{ee} is the J/ψ e^+e^- partial width (including vacuum polarization effects). The ISR kernel, to lowest order in the fine structure constant α, is

$$W(s,x) \equiv \frac{2\alpha}{\pi x}\left(\ln\frac{s}{m_e^2} - 1\right)\left(1 - x + \frac{x^2}{2}\right) \ , \tag{2}$$

in which m_e is the electron mass. The Breit-Wigner function is $b(s') \equiv B(s')/\mathcal{B}_{\mu\mu}\Gamma_{ee}$,

$$B(s') \equiv \frac{12\pi\mathcal{B}_{\mu\mu}\Gamma_{ee}\Gamma_{\rm tot}}{(s'-M^2)^2+M^2\Gamma_{\rm tot}^2} \ , \tag{3}$$

where $\Gamma_{\rm tot}$ is the full width and M the J/ψ mass.

The cross section $\sigma_0 \equiv \sigma(s_0)$ for $e^+e^- \to \gamma J/\psi \to \gamma\mu^+\mu^-$ over a specified dimuon mass range can be obtained from Eq. (1) and measured:

$$\sigma_0 = \frac{N_{J/\psi} - N_{\rm bgd}}{\epsilon \times \mathcal{L}} = \Gamma_{ee} \times \mathcal{B}_{\mu\mu} \times I_0 \ , \tag{4}$$

in which $N_{J/\psi}$ is the number of signal events counted, $N_{\rm bgd}$ is the estimated background, ϵ is the detection efficiency obtained from Monte Carlo (MC) simulation, $I_0 \equiv I(s_0)$, and the integral

$$I(s) \equiv \int W(s,x)\ b(s')\ dx \tag{5}$$

is effectively insensitive to the value of $\Gamma_{\rm tot}$. Hence a measurement of σ_0 can be combined with $\mathcal{B}_{\mu\mu}$ measurements [8] to yield $\Gamma_{ee}(J/\psi)$. For these equations to work, the number of events N and the integral above must both be determined with the same limits on x, which means the same limits on muon pair mass.

The above treatment ignores interference effects with the QED $\mu^+\mu^-$ production, which modify the dimuon mass lineshape asymmetrically around the peak; these effects are included at lowest order by replacing $B(s')$ with

$$B'(s') \equiv \frac{4\pi\alpha^2}{3s'}\left(\left|1-\frac{Q\,M\Gamma_{\rm tot}}{M^2-s'-iM\Gamma_{\rm tot}}\right|^2-1\right), \tag{6}$$

where $Q \equiv 3\sqrt{\mathcal{B}_{ee}\mathcal{B}_{\mu\mu}}/\alpha$.

Evaluation of Eq. (6) shows that interference is constructive above the peak and symmetrically destructive below, inducing a change in the Breit-Wigner cross section at $\sqrt{s} = M_{J/\psi} \pm \Gamma_{\rm tot}/2$, for example, of about $\pm 8\%$. At ± 300 MeV from the peak, the interference term induces an effect equal to $\pm 0.8\%$ of the nonresonant QED $\mu^+\mu^-$ cross section.

The integral $I(s)$ is performed numerically. The result for our $\sqrt{s}$=3.773 GeV dataset and x=0.139-0.488 (*i.e.*, $M(\mu^+\mu^-)$=2.8-3.4 GeV) is I_0=188.8$\pm$1.3 pb/keV using $W(s,x)$ from Eq. (2) and I_0=185.8$\pm$1.3 pb/keV when including the radiative corrections in Eq. (28) of Ref. [14]. Both values for I_0 include a net relative increase of $\sim$3% due to the interference term (using Eq. (6) instead of Eq. (3)), which occurs because the ISR kernel's $1/x$ term weights higher masses (constructive interference) more than lower masses (destructive interference). The quoted uncertainties on I_0 are based only on the statistics of the numerical integrations.

The event selection procedure is straightforward. The two highest-momentum tracks are required to have opposite charge, individually satisfy either $|\cos\theta|<0.83$ or $0.85<|\cos\theta|<0.93$ so as to avoid the barrel-to-endcap calorimeter transition region, and together have an invariant mass in the range 2.8-3.4 GeV. Bremsstrahlung photons, defined as calorimeter showers found within a 100 mrad cone about the initial charged track direction, are added to the corresponding Lorentz vector for the $M(\mu^+\mu^-)$ computation for each event. Muon pairs are loosely selected, and electrons effectively vetoed, by requiring the two

tracks to satisfy muon-like requirements on the matched energy-to-momentum ratio E/p: the larger of the two E/p values must be <0.5 and the smaller <0.25; electrons typically have $E/p \simeq 1$ and consistently satisfy $E/p > 0.5$. Cosmic rays are suppressed by requiring the pair of tracks together to point to within 2 mm of zero in the plane perpendicular to the beams and within 40 mm of zero along the beam direction. Cosmic rays are further suppressed by requiring the candidate J/ψ to have momentum $p_{\mu\mu} = 0.1$-1.5 GeV/c, a restriction which has no effect upon signal efficiency.

The dominant backgrounds to a $\gamma J/\psi$ signal are radiative returns to $\psi(2S)$ with subsequent decays $\psi(2S) \to XJ/\psi$. Such events will have a true $J/\psi \to \mu^+\mu^-$, but they will also tend to have extra tracks or showers, as well as a significant mass recoiling against the muon pair. Three requirements are imposed to suppress these events: one on extra charged tracks, a second on extra calorimeter showers, and a third on missing mass. The number of tracks satisfying loose quality criteria is required to be exactly two. The missing mass, $|p_{\rm cm} - (p_{\mu^+} + p_{\mu^-})|$, where $p_{\rm cm}$ is the initial state center-of-mass Lorentz vector, and p_{μ^+} and p_{μ^-} are the two muon Lorentz vectors, is required to be less than 500 MeV; this value is set by the need to reject both charged and neutral $\pi\pi J/\psi$ events. We search for the most energetic shower unassociated with a charged track that is not within a 100 mrad cone of either the initial momentum direction of either track or of the opposite of the net muon pair momentum direction, and demand it to have energy below 150 MeV. Figure 1 shows the two variables sensitive to backgrounds from radiative returns to $\psi(2S)$ for signal and $\gamma\psi(2S) \to \gamma XJ/\psi$, $J/\psi \to \mu^+\mu^-$ MC, demonstrating that the restrictions on extra showers and missing mass separate the signal from these backgrounds.

The `EvtGen` event generator [17], which includes final state radiation (FSR) [18], and a GEANT-based [13] detector simulation are used to study the radiative return (to J/ψ and $\psi(2S)$) processes with exactly one ISR photon. Events are generated with the polar angle distribution from Ref. [16], and account for ISR according to Eqs. (1-3). Non-resonant events of the type $\gamma(\gamma...)\mu^+\mu^-$ are generated from the Babayaga [12] package, which, unlike the radiative return process of `Evtgen`, includes the effects of multiple ISR and/or FSR photon emission, and hence of higher orders in α. The Babayaga code normally includes the interference effects with J/ψ decays, but this feature was removed for the results shown here.

In the absence of an MC generator package incorporating multiple photon emission from the initial state and from J/ψ decays in the radiative return process, we calculate the efficiency of the J/ψ signal in three steps, assuming that ISR and decay radiation are factorizable. For the first step, in order to simulate production of $\gamma(\gamma...)J/\psi \to \gamma(\gamma...)\mu^+\mu^-$, we use a subset of Babayaga-generated $e^+e^- \to \gamma(\gamma...)\mu^+\mu^-$ events with FSR disabled and a muon pair mass (including photons emitted within 100 mrad of either muon's direction) restricted to within ± 10 MeV of $M_{J/\psi}$. After detector simulation and reconstruction, 73.2% of such events pass our selection criteria. For the second step, we compare the `EvtGen` efficiency with J/ψ decay radiation from PHOTOS [18] to that without it, finding that decay radiation reduces the efficiency by factor of 0.968. The third step accounts for imperfections in modeling track-finding and decay radiation, for which we correct the efficiency by the factor 0.995 [19], arriving at ϵ=70.5%.

In order to probe both the background levels as well as the modeling of the largest shower and missing mass restrictions, we also perform the analysis with two alternate sets of selection criteria, differing from nominal only in that for the "loose" ("tight") set, we require the highest energy shower to have energy less than 200 MeV (100 MeV), and that

the missing mass be less than 550 MeV (450 MeV). These variations result in a relative efficiency change of +1.6% (−1.9%).

Table I shows the expected number of background events from $\gamma\psi(2S) \to \gamma X J/\psi$, $J/\psi \to \mu^+\mu^-$, and from $\gamma J/\psi$, $J/\psi \to \pi^+\pi^-$. The total number is 1.3% of the signal. For the alternate "loose" ("tight") selection, the relative background prediction is 5% (0.5%). Other J/ψ decay modes are found to contaminate our sample at negligibly small levels. No other processes will produce a peak at the J/ψ mass. Other backgrounds are assumed to be smooth in $M(\mu^+\mu^-)$ and fittable by a low-order polynomial.

In order to avoid depending on near-perfect MC simulation of the mass resolution, an alternate procedure is used to generate an accurate expected shape of the dimuon mass spectrum. We take a clean sample of $J/\psi \to \mu^+\mu^-$ decays from *data* in which there is no interference and convolve the measured mass resolution with the expected effects from interference to obtain the expected shapes. CLEO has already accumulated a large sample of essentially background-free radiative return events from $\sqrt{s}$=3.773 GeV to $\psi(2S)$, $\psi(2S) \to \pi\pi J/\psi \to \pi\pi\mu^+\mu^-$ [7], with almost the same selection criteria as for this analysis. After rejecting events failing the 150 MeV unaffiliated shower veto, we take the mass distribution from these 11,305 events, summed over both the charged and neutral dipion samples, and offset it by $M_{J/\psi}$ so as to be peaked at zero. The resulting distribution is taken to represent the mass resolution function in the 2.8-3.4 GeV mass region. In a toy MC, three different mass distributions are generated for dimuons with ISR: from a J/ψ decay alone (Eq. (3)), from non-resonant first-order QED, $e^+e^- \to \gamma\mu^+\mu^-$ ($4\pi\alpha^2/3s'$), and for the combination including interference ($4\pi\alpha^2/3s' + B'(s')$). For each "event" in each distribution, the mass is smeared according to the mass resolution function from $\gamma\psi(2S)$ data and recorded in a histogram. The final step is the subtraction of the properly normalized QED-only nonresonant mass distribution from that for QED-plus-J/ψ-with-interference to obtain the expected shape of the J/ψ mass peak from radiative returns. We designate this expected shape of the J/ψ peak including resolution and interference as $H(M_i)$, which has the property $\sum_i H(M_i) = 1$, where M_i is the center of the ith mass bin.

The following approach is taken for fitting the smooth non-resonant background: in seven fits from the widest window (2.8-3.4 GeV) to the narrowest (3.06-3.14 GeV), the lowest order polynomial is used that, in combination with the signal shape from above, gives at least a 1.0% confidence level (CL) for the fit. In practice, this meant using a third order polynomial for ranges wider than 2.9-3.3 GeV, a linear background for ranges narrower than 3.03-3.17 GeV, and a second order polynomial otherwise. We chose this strategy to allow for statistical fluctuations in the signal resolution function, to avoid introduction of an unphysical background shape, and to maximize the orthogonality of the signal and background functions. The fitting function is

$$f(M_i) = N_{J/\psi} H(M_i) + \Delta M \sum_{j=0}^{3} a_j (M_i - M_{J/\psi})^j, \tag{7}$$

where $N_{J/\psi}$ and a_j are the floating fit parameters, ΔM is the bin width, and, depending on the range, a_2 and/or a_3 can be set to be zero.

The normalization scheme represented in Eq. (4) will be referred to as the efficiency (E) method. The important features of the efficiency method are that one makes no assumptions about the composition of the non-resonant background, and that it requires an absolute efficiency measurement for the selection applied as well as absolute luminosity. An alternate normalization scheme, which will be referred to as the ratio (R) method, can be employed

to probe several systematic effects. In the ratio method (which was used in Ref. [3]), instead of using luminosity measured with e^+e^-, $\gamma\gamma$, and $\mu^+\mu^-$ events, we use the number of non-resonant $e^+e^- \to \gamma\mu^+\mu^-$ events underneath the J/ψ signal in the muon pair mass distribution. This alternate integrated luminosity is

$$\mathcal{L}_{\rm R} = \frac{N_{\rm QED}}{\epsilon_{\rm QED}\,\delta_{\rm QED}}\,, \tag{8}$$

in which $N_{\rm QED}$ is the number of non-resonant $\gamma\mu^+\mu^-$ events per unit mass from QED alone, evaluated at the J/ψ mass (which in terms of our fit is by definition the parameter a_0 from Eq. (7)), $\epsilon_{\rm QED}$ is the efficiency for non-resonant QED muon pair events to pass the selections, and $\delta_{\rm QED}$ is the cross section per unit mass predicted by non-resonant QED alone, without detector effects or selections, at $M{=}M_{J/\psi}$, including final state radiation and vacuum polarization effects. The value for $\delta_{\rm QED}$ is obtained by fitting the non-resonant $e^+e^- \to \gamma\mu^+\mu^-$ MC mass distribution at the generator level with the polynomial portion of Eq. (7) only, and dividing by the effective luminosity of the MC sample; we find $\delta_{\rm QED}{=}0.8510{\pm}0.0031$ pb/MeV for the Babayaga generator and a value 1.7% smaller when using a first-order (at most, one photon per event) generator [20]. We compute $\epsilon_{\rm QED}$ as in the first and third steps of that for ϵ, but with Babayaga FSR enabled, finding $\epsilon_{\rm QED}{=}69.2\%$.

The ratio method has, in place of Eq. (4),

$$\left(\frac{N_{J/\psi} - N_{\rm bgd}}{a_0}\right)\left(\frac{\epsilon_{\rm QED}}{\epsilon}\delta_{\rm QED}\right) = \Gamma_{ee} \times \mathcal{B}_{\mu\mu} \times I_0\ . \tag{9}$$

The ratio $\epsilon_{\rm QED}/\epsilon$ is expected to be close to unity; systematic effects which mostly cancel in this ratio include those from trigger, reconstruction, radiative corrections, and event selection variable modeling. The ratio method replaces systematics associated with the standard luminosity measurement and absolute efficiency determination with those applicable to a_0 and $\delta_{\rm QED}$. We note that $N_{J/\psi}$ and a_0 are almost completely anti-correlated, for which we account in the uncertainty propagation.

Unlike the efficiency method, the ratio method requires understanding non-J/ψ backgrounds, *i.e.,* the extent to which other final states besides radiative muon pairs populate the non-resonant entries in the mass distribution. Based upon measured cross sections [21] and MC studies of low-multiplicity hadronic final states, we conclude that all other backgrounds are negligible and assign an uncertainty of 0.3% in $\mathcal{B}_{\mu\mu} \times \Gamma_{ee}$ from this source.

Fits over all mass ranges strongly prefer the shape that includes interference to those which do not. This preference for the 2.9-3.3 GeV fit range, as shown with interference in Fig. 2(a) and without in Fig. 2(b), is a 6.6σ effect, as determined from the difference in log-likelihoods from the respective fits. The no-interference fit also systematically underestimates the yield by $\sim$3%, which, not coincidentally, is the amount by which interference changes the overall rate from 2.8-3.4 GeV.

Table II lists the quantities relevant to the $\mathcal{B}_{\mu\mu}{\times}\Gamma_{ee}$ measurements. Central values and statistical uncertainties of $N_{J/\psi}$ and a_0 are taken as unweighted means over the seven fits previously described, which have CL's ranging from 1-18%. Combining information from fits over different mass ranges in this manner samples different relative weightings of background and signal regions. The systematic errors on $N_{J/\psi}$ and a_0 are taken as the rms spreads of the corresponding fit results. The values from the efficiency and ratio methods are consistent within their uncorrelated uncertainties. The polynomial fits and shape agree very well with the luminosity-normalized expectation from the radiative muon pair MC.

For the efficiency method, the "loose" ("tight") selections induce changes in $\mathcal{B}_{\mu\mu} \times \Gamma_{ee}$ from nominal of +0.5% (−0.0%); similarly, the ratio method variation is +0.0% (+0.3%). These small changes demonstrate a good understanding of efficiency and background levels, which are reflected in their systematic errors in Table II.

The systematic errors on efficiency for the dimuon pair arise by extrapolating errors from the CLEO $\psi(2S) \to XJ/\psi$ analysis [19] as appropriate. Quoted errors for $I(s)$ and $\delta_{\rm QED}$ include, in addition to MC statistical uncertainties, contributions of 0.5% to account for accuracy of the underlying formulae. The systematic error on $N_{J/\psi}$ (or $N_{J/\psi}/a_0$) from fitting, computed as described above, is 0.9% (or 1.8%). The accuracy of the fitting assumptions is tested by pursuing the fitting procedure using MC $\gamma\psi(2S) \to \gamma\pi^+\pi^-\mu^+\mu^-$ events for the fitting shape, MC $\gamma J/\psi$ events, without any interference, for signal, and MC $\gamma\mu^+\mu^-$ for non-resonant background, all with statistics much larger than those of the data. From these high statistics samples, we find that the above procedure introduces a bias in $\mathcal{B}_{\mu\mu} \times \Gamma_{ee}$ of 1.0% for the efficiency method and 1.1% for the ratio method, both in the upward direction. We fully correct for these biases and assign a 0.7% systematic error to the corrections. The relative uncertainty attributable to the statistics of the resolution function in the data was estimated as follows. An ensemble $\gamma\psi(2S) \to \gamma\pi^+\pi^-\mu^+\mu^-$ MC samples was formed, each of the same size as the corresponding sample from the data, and each was used as the resolution function for the high-statistics MC muon pair distribution. The relative rms variation of the fit results for $N_{J/\psi}$ (a_0) for the ensemble was found to be 0.7% (0.8%), which is included as an additional systematic uncertainty. If, instead of adding the fitting systematic errors described above, we scale up the statistical errors by the square root of the reduced-χ^2 on each of the seven fits, similar total uncertainties are obtained, indicating reasonable error assignments.

Reference [3] asserts that $\epsilon_{\rm QED}/\epsilon \equiv 1$ and that the ratio method is insensitive to radiative corrections; we find neither to be the case for our analysis due to FSR effects. The ratio $\delta_{\rm QED}/I_0$ changes by ∼5% when ignoring radiative corrections: when both ISR and FSR are allowed, non-resonant events move from higher muon pair mass to lower mass, resulting in a net increase in events at $M = M_{J/\psi}$, whereas decay radiation in $J/\psi \to \mu^+\mu^-$ can only shift events out of the signal peak to lower masses.

We compute an error-weighted average of the E and R methods, accounting for correlations. While the ratio method avoids some of the systematics of the efficiency method, it suffers a larger fitting error, because $N_{J/\psi}$ is almost fully anti-correlated with a_0 (which is the non-resonant muon pair level at $M_{J/\psi}$). This average gives relative weights of 8:1 for E:R. The weighted average is $\mathcal{B}_{\mu\mu}\times\Gamma_{ee}$=0.3384±0.0058±0.0071 keV. For $\mathcal{B}_{\mu\mu}$ we use the CLEO measurement [8] $\mathcal{B}_{\ell\ell}$=(5.953±0.056±0.042)%, yielding Γ_{ee}=5.68±0.11±0.13 keV, and $\Gamma_{\rm tot}$=95.5±2.4 ± 2.4 keV. In all cases the first errors quoted are statistical and the second systematic, and the distinction between the two has been preserved in the propagation of uncertainties in $\mathcal{B}_{\ell\ell}$ to Γ_{ee} and $\Gamma_{\rm tot}$.

This measurement of $\mathcal{B}_{\mu\mu} \times \Gamma_{ee}$ is consistent with the BaBar [3] value, and the values determined here for Γ_{ee} and $\Gamma_{\rm tot}$ are more precise and somewhat larger than all previous measurements.

In summary, we have used the radiative return process $e^+e^-\to\gamma J/\psi$ to measure $\mathcal{B}_{\mu\mu}\times\Gamma_{ee}$ with a 2.7% relative uncertainty, and combined this with a CLEO measurement of $\mathcal{B}_{\ell\ell}$ to obtain Γ_{ee} (3.0%) and $\Gamma_{\rm tot}$ (3.6%) with improved precisions. Combining with $\Gamma_{ee}[\psi(2S)]$ = 2.54±0.03±0.11 keV from Ref. [7] and accounting for common uncertainties of luminosity, $\mathcal{B}_{\ell\ell}$, and lepton tracking, we determine $\Gamma_{ee}[\psi(2S)]/\Gamma_{ee}(J/\psi)$=0.45±0.01±0.02 (5.0%), a

quantity which might be more precisely predictable in LQCD than either Γ_{ee} alone.

We gratefully acknowledge the effort of the CESR staff in providing us with excellent luminosity and running conditions. A. Ryd thanks the A.P. Sloan Foundation. This work was supported by the National Science Foundation and the U.S. Department of Energy.

---

[1] N. Brambilla *et al.*, arXiv:hep-ph/0412158 (2004), unpublished.
[2] HPQCD and UKQCD Collaborations, A. Gray *et al.*, Phys. Rev. **D** 72, 094507 (2005).
[3] BaBar Collaboration, B. Aubert *et. al.*, Phys. Rev. D **69**, 011103(R) (2004).
[4] Particle Data Group, S. Eidelman *et al.*, Phys. Lett. **B592**, 1 (2004).
[5] BES Collaboration, J.Z. Bai *et al.*, Phys. Rev. D **58**, 092006 (1998).
[6] CLEO Collaboration, J.L. Rosner *et al.*, arXiv:hep-ex/0512046 (2005) (submitted to Phys. Rev. Lett.).
[7] CLEO Collaboration, N.E. Adam *et al.*, arXiv:hep-ex/0508023 (2005) (submitted to Phys. Rev. Lett.).
[8] CLEO Collaboration, Z. Li *et al.*, Phys. Rev. **D** 71, 111103(R) (2005).
[9] CLEO Collaboration, Y. Kubota *et al.*, Nucl. Instrum. Methods Phys. Res., Sect. A **320**, 66 (1992); D. Peterson *et al.*, Nucl. Instrum. Methods Phys. Res., Sect. A **478**, 142 (2002); M. Artuso *et al.*, Nucl. Instrum. Methods Phys. Res., Sect. A **554**, 147 (2005).
[10] CLEO-c/CESR-c Taskforces & CLEO-c Collaboration, R.A. Briere *et al.*, Cornell LEPP preprint CLNS 01/1742 (2001), unpublished.
[11] CLEO Collaboration, G. Crawford *et al.*, Nucl. Instrum. Methods Phys. Res., Sect. A **345**, 429 (1994).
[12] C.M. Carloni Calame *et al.*, Nucl. Phys. Proc. Suppl. B **131**, 48 (2004).
[13] R. Brun *et al.*, GEANT 3.21, CERN Program Library Long Writeup W5013 (1993), unpublished.
[14] E.A. Kuraev and V.S. Fadin, Sov. J. Nucl. Phys. **41**, 466 (1985).
[15] J.P. Alexander *et al.*, Nucl. Phys. **B320**, 45 (1989).
[16] G. Bonneau and F. Martin, Nucl. Phys. **B27**, 381 (1971); M. Benayoun *et al.*, Mod. Phys. Lett. **A14**, 2605 (1999).
[17] D.J. Lange, Nucl. Instrum. Methods Phys. Res., Sect. A **462**, 152 (2001).
[18] E. Barberio and Z. Was, Comput. Phys. Commun. **79**, 291 (1994).
[19] CLEO Collaboration, N.E. Adam *et al.*, Phys. Rev. Lett. **94**, 232002 (2005).
[20] F. Berends, R. Kleiss, and S. Jadach, Nucl. Phys. **B** 202, 63 (1982).
[21] CLEO Collaboration, N.E. Adam *et al.*, Phys. Rev. Lett. **94**, 012005 (2005); CLEO Collaboration, G.S. Adams *et al.*, Phys. Rev **D** 73, 012002 (2006); CLEO Collaboration, T.K. Pedlar *et al.*, Phys. Rev. Lett. **95**, 261803 (2005).

TABLE I: Number of background events expected.

Source	# Events
$\gamma J/\psi$, $J/\psi \to \pi^+\pi^-$	17.2
$\gamma\psi(2S) \to \gamma\pi^+\pi^- J/\psi$, $J/\psi \to \mu^+\mu^-$	6.2
$\gamma\psi(2S) \to \gamma\pi^0\pi^0 J/\psi$, $J/\psi \to \mu^+\mu^-$	62.4
$\gamma\psi(2S) \to \gamma\eta J/\psi$, $J/\psi \to \mu^+\mu^-$	2.1
$\gamma\psi(2S) \to \gamma\pi^0 J/\psi$, $J/\psi \to \mu^+\mu^-$	12.0
$\gamma\psi(2S) \to \gamma\chi_{c0}$, $\chi_{c0} \to \gamma J/\psi$, $J/\psi \to \mu^+\mu^-$	0.5
$\gamma\psi(2S) \to \gamma\chi_{c1}$, $\chi_{c1} \to \gamma J/\psi$, $J/\psi \to \mu^+\mu^-$	18.6
$\gamma\psi(2S) \to \gamma\chi_{c2}$, $\chi_{c2} \to \gamma J/\psi$, $J/\psi \to \mu^+\mu^-$	49.6
Total	168.7

TABLE II: Intermediate and final results for the efficiency (E) and ratio (R) methods, with statistical and systematic errors.

Quantity	Value
$N_{J/\psi}$	$12742 \pm 202 \pm 143$
$N_{\rm bgd}$	169 ± 9
I_0 (pb/keV)	185.8 ± 1.6
Efficiency (E) method	
ϵ (%)	70.5 ± 1.2
$\mathcal{L}$ (pb^{-1})	280.7 ± 2.8
Bias Factor	0.990 ± 0.007
$\mathcal{B}_{\mu\mu} \times \Gamma_{ee}$ (keV)	$0.3385 \pm 0.0054 \pm 0.0075$
Ratio (R) method	
a_0 (MeV^{-1})	$165.7 \pm 1.6 \pm 2.1$
$\epsilon_{\rm QED}/\epsilon$	0.981 ± 0.008
$\delta_{\rm QED}$ (pb/MeV)	0.8510 ± 0.0052
$\mathcal{L}_{\rm R}$ (pb^{-1})	281.5 ± 5.3
Bias Factor	0.989 ± 0.007
$\mathcal{B}_{\mu\mu} \times \Gamma_{ee}$ (keV)	$0.3373 \pm 0.0087 \pm 0.0096$

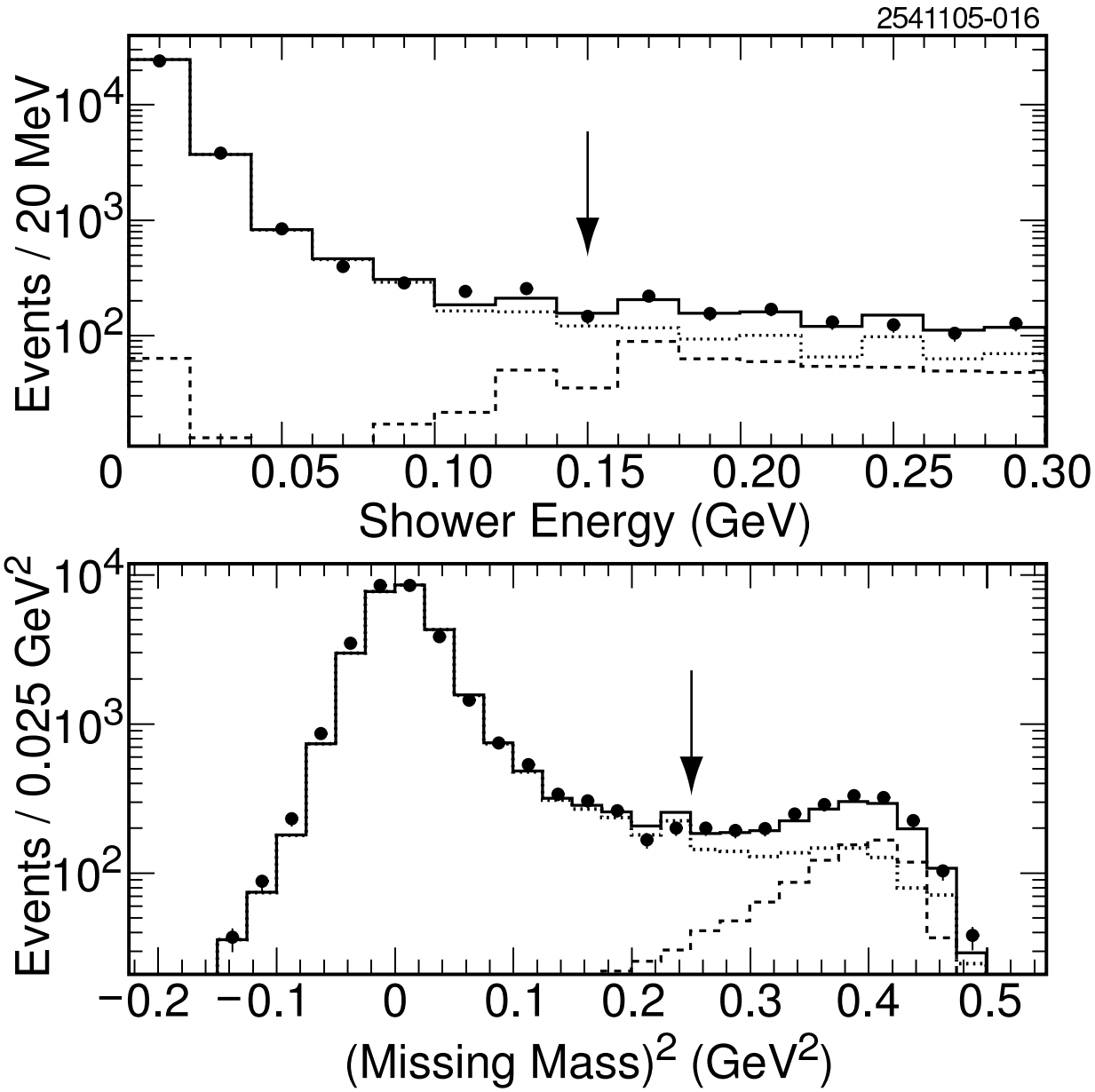

FIG. 1: Distributions, for $M_{\mu\mu}$=3.05-3.15 GeV, of the largest calorimeter shower energy unaffiliated with a charged track (top) and missing-mass-squared (bottom) for the data (filled circles), in the signal $\gamma J/\psi$ MC (dotted line histogram), $\gamma\psi(2S) \to \gamma X J/\psi$ MC (dashed), and their sum (solid). Arrows show the nominal upper limits of values accepted by the event selection.

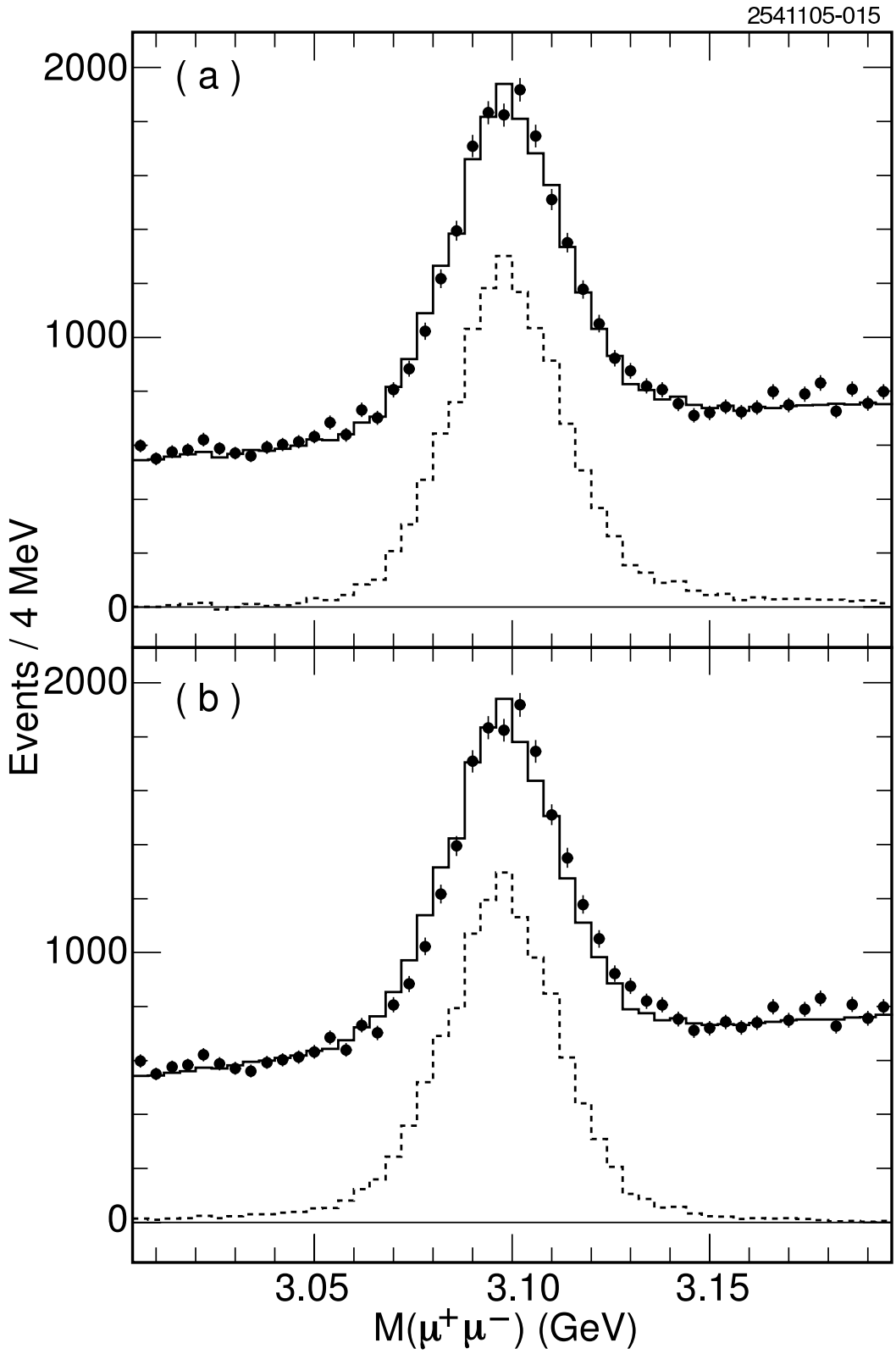

FIG. 2: Fit (solid line) of the muon pair invariant mass data (filled circles) to the sum of the expected shape (dashed line) for a J/ψ decay (a) with and (b) without interference combined with a smooth background (second order polynomial).